Dynamic Characterization of Bi-material Cantilevers

R Bijster, J de Vreugd, H Sadeghian
Department of optomechatronics
TNO
The Netherlands
Email: Hamed.SadeghianMarnani@tno.nl

***Abstract*—In this paper, an experimental-theoretical method is proposed to accurately determine the thermal diffusivity, characteristic time constant and layer thicknesses of a bi-material cantilever using a transient, non-destructive and non-contact measurement. The technique is based on the well-known optical beam deflection method. A time dependent, sinusoidal heat load is locally applied to induce a time varying thermal profile over the length of the beam, resulting in a mismatch-strain between the two layers that bends the cantilever. A measurement of the phase difference between the thermo-mechanical response and the input signal can be used to extract the thermal diffusivity, characteristic time constant and the location of the heat source. For this reason a closed-form analytical solution for the thermo-mechanical response is presented. The dynamic response of the system is characterized using the transfer function in the Laplace domain. The analytical solution includes a Gaussian distributed, time-dependent heat source of known width at a location along the beam. A constant convective heat transfer coefficient can be included to allow measurement in ambient conditions. A combination of a measurement of the thermal diffusivity and the effective conductance are used to calculate the mutual layer thicknesses of the two layers.**

Keywords-bilayer cantilevers; characterization; diffusivity.

I. INTRODUCTION

Bi-material cantilevers are widely used in nano-instrumentation as actuators and sensors. The material properties and geometry of these cantilevers vary largely between batches and are not well controlled. In this paper, a method is proposed to accurately determine the thermal diffusivity, effective conductance and layer thicknesses by means of a transient, non-destructive, non-contact measurement. This allows quick characterization of bi-material cantilevers, e.g., after production or for acceptance testing.

II. THEORY

The thermal diffusivity is a measure for the velocity at which heat spreads throughout a medium, e.g., a micro-cantilever. It cannot be measured directly and needs to be determined through a proxy. In this derivation, it is assumed that a cantilever beam is concerned, although the derivation could equally well be performed for other boundary conditions. The cantilever is assumed to be heated locally with a Gaussian power distribution (e.g. by using a laser). This is typical for the optical beam deflection method, popular in Scanning Probe Microscopy setups. The heating results in a temperature distribution over the length of the beam. It is assumed, that the temperature distribution over the thickness of the cantilever is negligible. The temperature distribution over the length of the cantilever causes a mismatch strain on the interface between the two layers of the cantilever due to the unequal expansion coefficients of the materials. The mismatch strain results in a bending of the cantilever. If the input signal is varied sinusoidally, the cantilever will oscillate at the same frequency. The rotation at a specific location, however, will lag behind with respect to the input signal. This phase shift is caused by the thermal diffusivity and is dependent on spot position and input frequency. The relation between these variables will be derived in the following sections.

A. Temperature distribution

The temperature distribution along the length of the beam is dominated by the heat equation. This heat equation can be formulated in its most general form as

$$\frac{\partial T(x,t)}{\partial t} = D\frac{\partial^2 T(x,t)}{\partial x^2} - B\left(T(x,t) - T_{env}\right) + f(x,t) \tag{1}$$

where $T(x,t)$ is the temperature along the beam in Kelvin, x is the running coordinate along the length ($x = 0$ at the base, $x = L$ at the tip), D is the thermal diffusivity in $\mathrm{m}^2\,\mathrm{s}^{-1}$, B is the characteristic time constant for convective heat transfer in s^{-1} and $f(x,t)$ is a heat source function. The environment is defined by means of two non-zero boundary conditions(e.g. a Dirichlet boundary condition at the base and a Neumann boundary conditions at the tip) including a non-zero initial condition. To simplify the solution of (1) a change of variables is used. When it is assumed that the base temperature is constant and equal to the environmental temperature T_{env}, one can define

$$u(x,t) = T(x,t) - T_{env} \tag{2}$$

With this change in variables both boundary conditions and the initial condition can be set to zero when required and the equation reduces to

$$u_t = Du_{xx} - Bu + f(x,t) \tag{3}$$

 ISBN: 978-1-61208-297-4

This is a realistic assumption for most microcantilevers, because these are often mounted on a base that is far greater in dimensions and heat capacity. The transformed equation has to meet the following boundary and initial conditions:

$$u(0,t) = u_x(L,t) = u(x,0) = 0 \tag{4}$$

It is assumed, that the source function can be described with

$$f(x,t) = a(t) \exp\left(-\frac{(x-b)^2}{2c^2}\right) \tag{5}$$

where a is a term in $\mathrm{W\,m^{-1}}$ that determines the amplitude of the distribution, b is the coordinate of the center position of the spot and c is a constant that determines the width of the spot. The constant c is related to the Full-Width Half Maximum of the beam as follows from (6)

$$c = \frac{FWHM}{2\sqrt{2\ln 2}} \tag{6}$$

Using a Gaussian distribution gives a good representation of the physical laser spot. The problem can be solved using the Method of Laplace. Taking the Laplace transform of (3) results in the following ODE

$$\frac{\partial^2 \tilde{u}}{\partial x^2} - \frac{s+B}{D}\tilde{u} = -\frac{\tilde{f}}{D} \tag{7}$$

where $\tilde{u}$ and $\tilde{f}$ are the Laplace transformed function of $u(x,t)$ and source function $f(x,t)$ respectively. The amplitude of the signal can be a function of time, while the position of the source is assumed constant. This implies that the source function can be written as

$$\tilde{f} = \tilde{F}(s) \cdot \exp\left(-\frac{(x-b)^2}{2c^2}\right) \tag{8}$$

The homogeneous solution for the ODE of (7) can be verified to be

$$\tilde{u}_c = c_1 \exp\left(\sqrt{\frac{s+B}{D}}\right) + c_2 \exp\left(-\sqrt{\frac{s+B}{D}}\right) = c_1\tilde{u}_1 + c_2\tilde{u}_2 \tag{9}$$

The particular solution can be found using the Method of Variation of Parameters in which the solution is expressed as a function of the fundamental solutions $\tilde{u}_1$ and $\tilde{u}_2$.

$$\tilde{u}_p = -\tilde{u}_1 \int \frac{\tilde{u}_2 \tilde{g}}{W(\tilde{u}_1, \tilde{u}_2)} dx + \tilde{u}_2 \int \frac{\tilde{u}_1 \tilde{g}}{W(\tilde{u}_1, \tilde{u}_2)} dx \tag{10}$$

where W is the Wronskian of the fundamental solutions

$$W(\tilde{u}_1, \tilde{u}_2) = \tilde{u}_1\tilde{u}_2' - \tilde{u}_2\tilde{u}_1' \tag{11}$$

and $g(x) = -\tilde{f}/D$. The general solution then becomes

$$\tilde{u} = c_1\tilde{u}_1 + c_2\tilde{u}_2 + \tilde{u}_p \tag{12}$$

where the constants can be solved for using the conditions of (4). Due to the complexity and length of the intermediate results, these equations have been solved using Maple algebraic software.

B. Rotation of the cantilever

The curvature of the beam can be given as a function of the geometry and the mismatch strain by

$$\kappa = \frac{\partial^2 z}{\partial x^2} = \beta \epsilon_m \tag{13}$$

with ϵ_m the mismatch strain, κ the beam curvature in m and z the out of plane displacement of the cantilever in m. The mismatch strain itself can be easily calculated as

$$\epsilon_m = \Delta\alpha\,(T(x) - T_{SFT}) \tag{14}$$

where $\Delta\alpha$ is the difference in thermal expansion coefficient of the used materials, $T(x)$ is the temperature along the beam and T_{SFT} is the Stress-Free Temperature. The constant β is a function of the geometry and material properties of the individial layers. It is defined using the following equations [1]:

$$\beta = \frac{6hm}{t_2}\left(\frac{1+h}{1+2hm\,(2+3h+2h^2)+h^4m^2}\right) \tag{15}$$

In this relation the following auxiliary parameters are defined:

$$h = \frac{t_1}{t_2} \tag{16}$$

$$m = \frac{M_1}{M_2} \tag{17}$$

$$M_i = \frac{E_i}{1-\nu_i} \tag{18}$$

where E is the Young's modulus of the material, t is the layer thickness, ν the Poisson ratio and the subscript i refers to the respective layer (1, top; 2, bottom). Integration with respect to x results in an expression for the rotation:

$$\tilde{\theta} = \beta\Delta\alpha \int \tilde{u}dx + \beta\Delta\alpha\,(T_{env} - T_{SFT})\,x + \theta_0 \tag{19}$$

The second term on the right hand side of this equation gives the static cantilever rotation due to the environmental conditions. In measurements this can easily be aligned for such that this term effectively becomes zero. In this case only the dynamic effects that influence the period and phase are considered, which reduces this equation to:

$$\tilde{\theta}_{dyn} = \int \tilde{u}dx + \theta_{0,dyn} \tag{20}$$

The term $\theta_{0,dyn}$ can be solved for using the boundary condition that the rotation at the base of the cantilever always has to be zero. The transfer function for the rotation of the cantilever due to a local heat input is given by (21).

 ISBN: 978-1-61208-297-4

$$G(s) = \frac{\sqrt{2\pi}c}{8(s+B)\cosh(k_3)}\{ - 2\exp(k_1)[\mathrm{erf}(\mathrm{m}_1) + \mathrm{erf}(\mathrm{m}_2)] + 2\exp(k_2)[\mathrm{erf}(\mathrm{m}_4) - \mathrm{erf}(\mathrm{m}_3)] + 4\cosh(k_3)\mathrm{erf}(\mathrm{m}_5) + \exp(k_4)[\mathrm{erf}(\mathrm{m}_3) - \mathrm{erf}(\mathrm{m}_4)] + \exp(k_5)[\mathrm{erf}(\mathrm{m}_2) + \mathrm{erf}(\mathrm{m}_4)] + \exp(k_6)[\mathrm{erf}(\mathrm{m}_3) - \mathrm{erf}(\mathrm{m}_1)] + \exp(k_7)[\mathrm{erf}(\mathrm{m}_1) + \mathrm{erf}(\mathrm{m}_2)]\} \quad (21)$$

The auxiliary terms in this equation are omitted here for brevity and can be found in the Appendix. The phase lag of

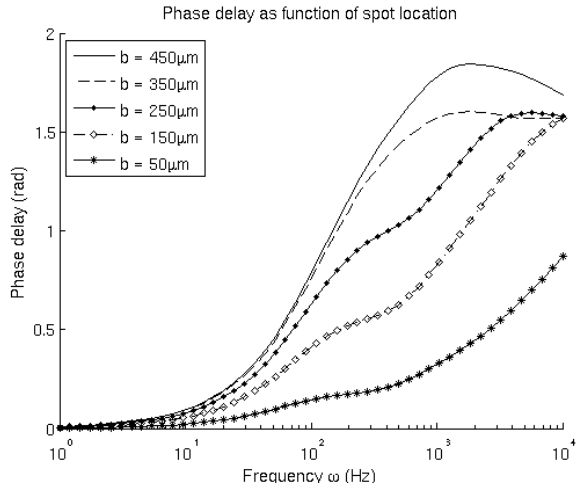

Figure 1. Phase shift as function of position. $L = 500$ µm, $D = 7 \cdot 10^{-5}$ m^2 s^{-1}, Full-Width Half Minimum of spot = 30 µm, spot location indicated in legend in µm.

the response with respect to the input is easily found from the transfer function by substituting $s = j\omega$. The argument of the complex output gives the phase angle. The phase lag for the rotation of the cantilever for a known location is depicted in Figure 1. Similarly the delay as a function of thermal diffusivity is plotted in Figure 2. Dependent on position and thermal diffusivity clearly distinct phase delays are found. With a proper initial guess of the parameters, for example based on manufacturer specifications, this allows for recovery of the thermal diffusivity by fitting the theoretical model to the measurement data.

C. Calculation of layer thicknesses

With traditional techniques, e.g., optical microscopy or Scanning Electron Microscopy (SEM), the thickness of a micro-cantilever cannot be measured with sufficient accuracy. The accuracy of these measurements is at approximately 1 µm in the same order of magnitude of the actual thickness. If the material properties are known (e.g. from

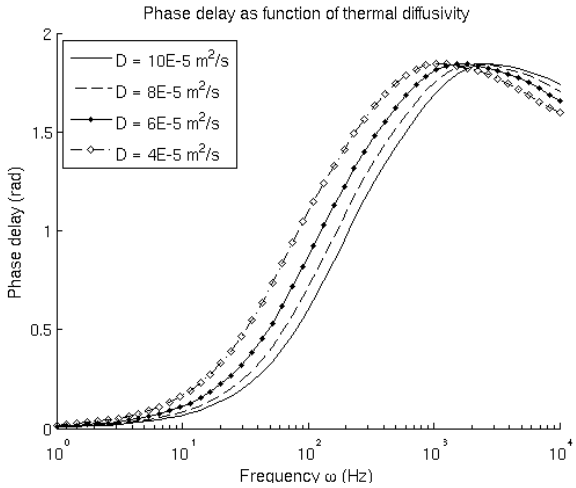

Figure 2. Phase shift as function of thermal diffusivity. $L = 500$ µm, Full-Width Half Minimum of spot = 30 µm, $b = 450$ µm. Thermal diffusivity is indicated in legend in m^2 s^{-1}.

measurement), equations can be derived with only the layer thicknesses as unknowns. One set of equations is given by the expressions for the thermal diffusivity D and the effective conductance G of a one-dimensional cantilever. The one dimensional heat equation can be written as

$$kAu_{xx} = c_p \rho A u_t \quad (22)$$

in which k is the thermal conductance in W m^{-1} K^{-1}, A is the cross-sectional area in m^2 and c_p is the specific heat capacity under constant pressure in J kg^{-1} K^{-1}. Assuming heat transfer mainly occurs in the longitudinal direction and is negligible in the other directions, the thermal conductance can be written in terms of the two layers as

$$kA = (k_1 t_1 + k_2 t_2)\, w \quad (23)$$

where w represents the width of the beam. The total heat capacity can then also be rewritten as a function of the two layers by

$$c_p \rho A = (c_{p,1}\rho_1 t_1 + c_{p,2}\rho_2 t_2)\, w \quad (24)$$

With the thermal diffusivity D defined by

$$D = \frac{k}{\rho c_p} \quad (25)$$

this results in the final expression for the thermal diffusivity

$$D = \frac{k_1 t_1 + k_2 t_2}{c_{p,1}\rho_1 t_1 + c_{p,2}\rho_2 t_2} \quad (26)$$

The effective conductance can also be expressed as a function of the two layer thicknesses using

$$G = (k_1 t_1 + k_2 t_2)\frac{w}{L} \quad (27)$$

Equations (26) and (27) form the required set that allows solving for the thicknesses, given that the thermal properties

of the layers are known. Solving the given system for the two mutual thicknesses results in the following expressions:

$$t_2 = \frac{GL\left(\frac{1}{D} - \frac{\rho_1 c_{p,1}}{k_1}\right)}{w\left(\rho_2 c_{p,2} - \frac{\rho_1 c_{p,1} k_2}{k_1}\right)} \tag{28}$$

$$t_1 = \frac{GL}{wk_1} - \frac{k_2}{k_1} t_2 \tag{29}$$

Assuming that the thermal diffusivity and effective conductance have been measured exactly and the material properties are known, the quality of the estimation of thicknesses via this method can be assessed. Here, cantilevers with a mono-crystalline silicon substrate and a gold reflective coating have been used. For these materials the material properties are known from literature within an accuracy of a few percent [2][3][4][5][6][7][8].

For this method, both the thermal diffusivity and the effective conductance need to be known. The thermal diffusivity is determined as explained earlier. The effective conductance can be determined as described below.
For a cantilever with the temperature distribution known when power is applied at the tip, the effective conductance can be expressed as

$$G = \frac{P}{\Delta T} \tag{30}$$

where G is the effective conductance in $\mathrm{W\,K^{-1}}$, P is the applied power in W and ΔT is the temperature difference between tip and base in K. Generally it is not possible to measure the tip temperature in an AFM setup and other means need to be used to find the effective conductance. One such method is described by Sheng, Narayanaswamy, Goh, and Chen[9], which use the changes in beam rotation caused by changes in the applied power and changes in the base temperature. In that scenario however, it is still assumed that the heat is applied at the tip of the cantilever. A similar analysis has been done for the general case in which the beam is heated locally at an arbitrary position along its length.

In the following derivation, it is assumed that the beam is locally heated by a laser with a Gaussian distributed spot as introduced earlier. Only the steady state solution will be considered. If vacuum conditions are assumed, the problem can be stated as

$$Du_{xx} + \frac{D}{\frac{k_1 t_1 + k_2 t_2}{t_1 + t_2}} \frac{P(x,t)}{(t_1 + t_2)\, w} = u_t \tag{31}$$

with $P(x,t)$ in $\mathrm{W\,m^{-1}}$. If one uses P_0 to represent the total power impinging on the cantilever, the term a can be derived from the forcing function using the following relation:

$$P_0 = \int_0^L a \exp\left(-\frac{(x-b)^2}{2c^2}\right) dx \tag{32}$$

Solving this equation for the term a results in

$$a = P_0 \left(1/2c\sqrt{2\pi}\left(\mathrm{erf}\left(\frac{\mathrm{b}}{\mathrm{c}}\frac{\sqrt{2}}{2}\right) + \mathrm{erf}\left(\frac{\mathrm{L\text{-}b}}{\mathrm{c}}\frac{\sqrt{2}}{2}\right)\right)\right)^{-1} \tag{33}$$

Because only steady state is considered the partial derivative with respect to time t equals zero. The problem then becomes a simple ODE that after repeated integration gives the temperature distribution over the beam. The ODE is reduced to

$$u_{xx} = -\frac{a}{\bar{k}} \exp\left(\frac{-(x-b)^2}{2c^2}\right) \tag{34}$$

with $\bar{k}$ defined as

$$\bar{k} = (k_1 t_1 + k_2 t_2)\, w \tag{35}$$

The two integration constants can be solved for by considering the boundary conditions of (4). The temperature distribution with respect to the base temperature is given by

$$\begin{aligned} u(x) = {} & \\ & - P_0 \left(\sqrt{2}c\left\{\exp\left(-\frac{(b-x)^2}{2c^2}\right) - \exp\left(-\frac{b^2}{2c^2}\right)\right\}\right. \\ & + \sqrt{\pi}\left\{(b-x)\,\mathrm{erf}\left(\frac{\sqrt{2}}{2}\frac{\mathrm{b\text{-}x}}{\mathrm{c}}\right) - x\,\mathrm{erf}\left(\frac{\sqrt{2}}{2}\frac{\mathrm{L\text{-}b}}{\mathrm{c}}\right)\right. \\ & \left.\left. - b\,\mathrm{erf}\left(\frac{\sqrt{2}}{2}\frac{\mathrm{b}}{\mathrm{c}}\right)\right\}\right) \\ & \Big/ \left\{\bar{k}\sqrt{\pi}\left(\mathrm{erf}\left(\frac{\sqrt{2}}{2}\frac{\mathrm{b}}{\mathrm{c}}\right) + \mathrm{erf}\left(\frac{\sqrt{2}}{2}\frac{\mathrm{L\text{-}b}}{\mathrm{c}}\right)\right)\right\} \end{aligned} \tag{36}$$

By defining $H \equiv \beta\Delta\alpha$ and using the earlier developed relations for the rotation of the cantilever, one can deduce that

$$\theta_r(x) = H \int u(x)\, dx + H\,(T_{env} - T_{SFT})\, x + c_3 \tag{37}$$

where the integration constant can be solved for by considering that the rotation at the base shall be zero and constant. Substituting $x = b$, for the rotation is measured at the location of actuation, results in the total mechanical response to be equal to (38).

 ISBN: 978-1-61208-297-4

$$\theta_r\left(x=b\right)=$$
$$H\left(P_0 b^2\sqrt{\pi}\left\{\operatorname{erf}\left(\frac{\sqrt{2}}{2}\frac{\text{L-b}}{\text{c}}\right)+\operatorname{erf}\left(\frac{\sqrt{2}}{2}\frac{\text{b}}{\text{c}}\right)\right\}\right.$$
$$2b\sqrt{\pi}\bar{k}\left(T_{env}-T_{SFT}\right)\left\{\operatorname{erf}\left(\frac{\sqrt{2}}{2}\frac{\text{b}}{\text{c}}\right)-\operatorname{erf}\left(\frac{\sqrt{2}}{2}\frac{\text{L-b}}{\text{c}}\right)\right\}$$
$$\left.-P_0\sqrt{\pi}c2\operatorname{erf}\left(\frac{\sqrt{2}}{2}\frac{\text{b}}{\text{c}}\right)-P_0 bc\sqrt{2}\exp\left(-\frac{b^2}{2c^2}\right)\right)$$
$$\Big/\left\{2\bar{k}\sqrt{\pi}\left(\operatorname{erf}\left(\frac{\sqrt{2}}{2}\frac{\text{b}}{\text{c}}\right)+\operatorname{erf}\left(\frac{\sqrt{2}}{2}\frac{\text{L-b}}{\text{c}}\right)\right)\right\} \quad (38)$$

By studying the change in beam rotation caused by a change in incident power and a change in base temperature two expressions can be derived to solve for the unknown constants H and $\bar{k}$. Expressions for these changes can be found using partial differentiation of (38) with respect to P_0 and T_{env} respectively. This results in the following set of relations.

$$\frac{\partial\theta_r\left(x=b\right)}{\partial P_0}=$$
$$H\left(b^2\sqrt{\pi}\left\{\operatorname{erf}\left(\frac{\sqrt{2}}{2}\frac{\text{L-b}}{\text{c}}\right)+\operatorname{erf}\left(\frac{\sqrt{2}}{2}\frac{\text{b}}{\text{c}}\right)\right\}\right.$$
$$+\left(b^2-c^2\right)\sqrt{\pi}\operatorname{erf}\left(\frac{\sqrt{2}}{2}\frac{\text{b}}{\text{c}}\right)+bc\sqrt{2}\exp\left(-\frac{b^2}{c^2}\right)\Big)$$
$$\Big/\left\{2\bar{k}\sqrt{\pi}\left(\operatorname{erf}\left(\frac{\sqrt{2}}{2}\frac{\text{b}}{\text{c}}\right)+\operatorname{erf}\left(\frac{\sqrt{2}}{2}\frac{\text{L-b}}{\text{c}}\right)\right)\right\} \quad (39)$$

$$\frac{\partial\theta_r\left(x=b\right)}{\partial T_{env}}=Hb \quad (40)$$

The position of the spot can be found in multiple ways and the thermal diffusivity can be derived from experiments as explained earlier. Combined with the found value for $\bar{k}$ one now has two functions of t_1 and t_2 that can be solved for: (26) and (35).

III. Experiments

The developed relations have been compared to experimentation. In this section the used setup and obtained results will be discussed.

A. Experimental setup

The setup implements the optical lever technique to actuate and measure the rotation of the beam. A sketch of the setup is given in Figure 3. A 633 nm (red) fiber laser is used. The beam passes through a collimator to obtain a collimated beam of 1.5 mm wide. The light then passes through a $\lambda/2$ waveplate to shift the polarization. In the polarizing beam splitter the light is partially reflected to the beam dump, the remaining light passes straight through. The amount that passes through is regulated using the waveplates. The light continues by passes through another $\lambda/2$ waveplate to change the polarization again. In the second polarizing beam splitter the light is reflected to a power meter and the rest passes on through a $\lambda/4$ waveplate that changes the polarization from linear to circular. The light is then focused on the cantilever using a $f = 20$ mm, $10\times$ microscope objective. Part of the power of the light is absorbed, changing the rotation of the beam. The light is reflected under a slight angle back into the microscope objective. On the way back, the light passes through the $\lambda/4$ waveplate again. Because the light has been reflected in the meantime, the polarization is now shifted by $90°$. The light is reflected by the polarizing beam splitter onto the OPS detector. The remaining light passes straight through and eventually ends up at the detector of the camera. The Maypa OPS is a linear Position Sensitive

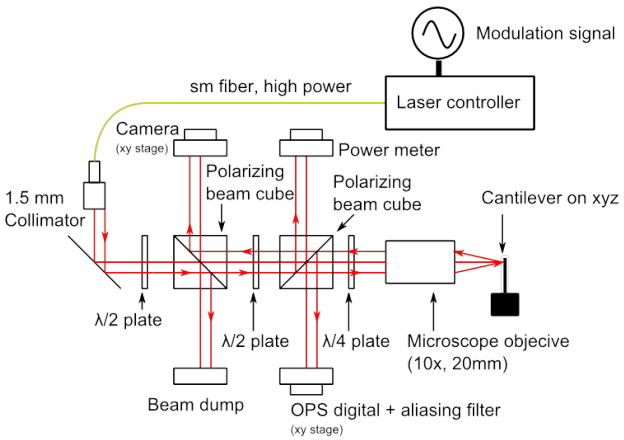

Figure 3. Schematic drawing of tabletop AFM setup[10].

Detector (PSD) that registers the position of the spot in a plane perpendicular to the incoming beam and its intensity. The OPS is mounted on an XY-stage that allows alignment of the sensor. The OPS is aligned such that at a given reference power level, the resulting rotation of the cantilever is set as datum. The camera present in the setup is used for optical alignment of the laser spot on the cantilever. The cantilever is mounted on an XYZ translational stage for this purpose. It can be used to move the laser spot along the cantilever and to get it into focus of the laser beam. More details regarding the tabletop AFM setup are given by Sadeghian et al. [10].

For the performed experiments the Nanoworld ARROW-TL8Au cantilevers have been used. These have a rectangular plan form with a triangular shaped end. The cross-section is rectangular and consists of a approximately 1 µm thick Silicon substrate and an approximately 30 nm Gold reflective

 ISBN: 978-1-61208-297-4

coating. The absence of a tip and the relatively high beam ratio of 5 make it a proper candidate for the validation of the theory. From discussions with the manufacturer it became clear that between the substrate and the reflective coating a third layer is added to prevent diffusion of the gold atoms into the silicon substrate. This intermediate layer has a thickness of approximately 4 nm and can be composed of either titanium or chromium. The actual used material is unknown. In the analysis, it is assumed that the effect of this layer is negligble compared to the thicker reflective coating and much thicker substrate. The dimensions of the cantilever plan form can be found in Figure 4. The accuracy of this measurement is 1 µm. Using SEM the thickness can therefore not be measured. The predicted thicknesses from theory can therefore not be validated against an absolute reference. Using the described setup, cantilevers can be

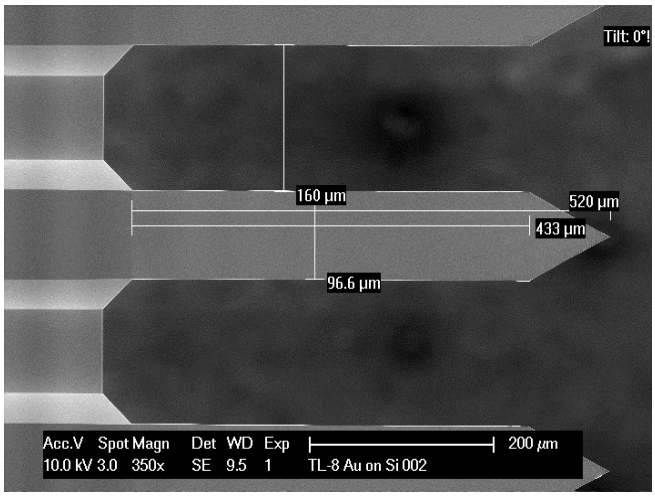

Figure 4. SEM of Nanoworld ARROW-TL8Au cantilevers used in measurements including dimensions.

actuated upto approximately 10 kHz. After that the signal to noise ratio (SNR) will become too low for registration of the movement of the cantilever.

B. Experimental procedure

The laser spot is placed in a required reference position by correlation of photographs taken using the microscope objective and CCD camera present in the setup with the SEM of the cantilever as depicted in Figure 5. After alignment the required laser power is set manually and the laser is focused. The OPS is aligned such that the returning laser beam hits it as close to its center as possible to reduce the effects of any sensor non-linearity. Any remaining sensor signal caused by the initial rotation of the cantilever is nulled in postprocessing. The setup is mounted on a pneumatically stabilized table and stored in a light tight container to reduce the effects of environmental vibration and stray light.

To determine the thermal diffusivity of the cantilever, the phase delay of the rotation with respect to the input signal is

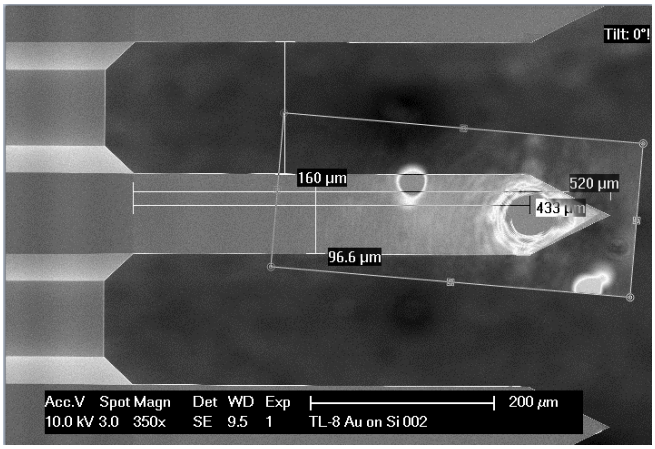

Figure 5. Alignment of the laser spot on the cantilever by correlation of CCD images with SEM of the cantilever.

measured. This is done by modulating the laser diode current sinusoidially. The mean current (I_{DC}) is set to the level that was also set after the detector alignment. The amplitude of the wave (I_{AC}) can be chosen freely, as long as the minimum and maximum currents as specified for the laser diode are not exceeded. The diode current is then modulated as

$$I_{LD} = I_{DC} + I_{AC} \sin(\omega_i t) \tag{41}$$

The frequency ω is set to several values on a logarithmic interval between 1 and $10,000$ Hz for the ARROW-TL8Au cantilevers. The acquisition time is dependent on the actuation frequency and is taken to cover at least ten full cycles with a minimum of 0.1 s. For the used cantilevers this is sufficient to reach a steady mean cantilever temperature. As the initial temperature is not known exactly, using temperature fluctuations around a steady mean negates the need for inclusion of the transient. A generic sine function is later fitted to the steady state cycles of the measured rotation and the phase shift is extracted.

C. Results

The phase angle is used to fit (21) to the processed delay measurements. It is assumed in this fit that the experiment was performed in vacuum and B is thus equal to zero. The found diffusivity is therefore an overestimate. However, as the error is systematic, the results can be used to judge the validity of the derived equations. This decision is justified by the large uncertainty in convective heat transfer coefficient. The convective time constant B can be related to the convective heat transfer coefficient via

$$B = \frac{hA}{mc_p} \tag{42}$$

where h is the heat transfer coefficient in $\mathrm{W\,m^{-2}\,K^{-1}}$, A is the area involved in convective heat transfer in $\mathrm{m^2}$ and the product $m \cdot c_p$ is the total heat capacity of the

cantilever in $\mathrm{J\,K^{-1}}$. The total heat capacity is unknown, as well as the exact area exposed to convective heat transfer. The convective heat transfer coefficient is unknown and values reported in literature vary largely. For example, Sheng, Narayanaswamy, Goh, and Chen[9] report values of $h = 500 - 5000\ \mathrm{W\,m^{-2}\,K^{-1}}$. The physics behind this large convective heat transfer coeffient is currently poorly understood [11][12]. For this reason it was decided to assume no convective heat transfer and accept the systematic error. Future experiments in vacuum are required for full validation of the theory.

In estimating the thermal diffusivity all frequencies between 1 and 2000 Hz were used. Higher frequencies were discarded because the mechanical resonance frequency of the cantilever dominated here. This effect was not covered in the developed theoretical model. The non-linear fitting procedure requires an initial guess for the thermal diffusivity. Based on manufacturer specifications the thermal diffusivity is assumed $D = 7 \cdot 10^{-5}\ \mathrm{m^2\,s^{-1}}$. The spot positions are obtained from correlation of the CCD camera images with the SEM of the cantilever. The found diffusivities are plotted as a function of the laser spot center position in Figure 6. As can be seen in the diagram,

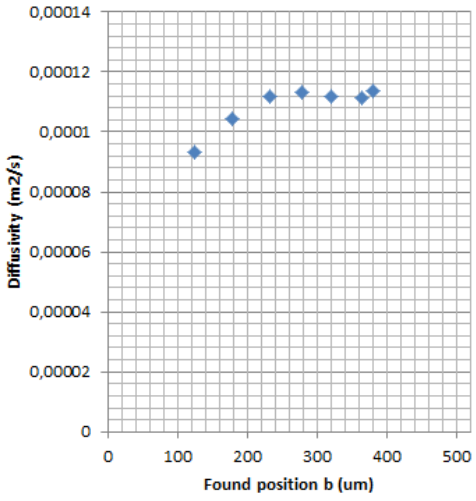

Figure 6. Found diffusivity as function of spot center position.

the variation of the estimation of the thermal diffusivity is small for a large range of spot center positions. However, when the spot gets closer to the base of the cantilever, the estimation of thermal diffusivity drops considerably. It is currently speculated that this is caused by a significant heat leak into the base causing the temperature of the base to change. This will have to be verified in future experiments. During measurements it was noticed that the extracted thermal diffusivity was dependent on the incident laser power. The incident mean laser power was set to $1.33, 2.00, 2.69$ and 3.26 mW. Per mean power setting, wave magnitudes of $0.3802, 0.7604$ and 1.1407 mW were superimposed. The found thermal diffusivities are plotted in Figure 7. As can be seen in Figure 7 the derived diffusivity

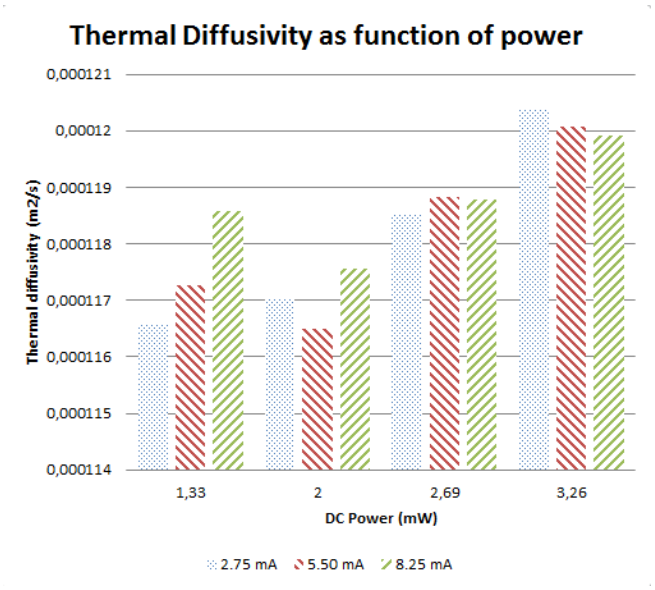

Figure 7. Found thermal diffusivity as a function of power, assuming vacuum conditions. Spot located at $b = 433$ µm.

varies with both AC power and DC power. No clear trend is evident from the results. Although at DC power settings of $1.33, 2.69$ and 3.26 mW a higher AC power seems to increase the estimate, although this is not true for 2.00 mW. Also the change in diffusivity does not seem to adhere any evident relation. The reasons for this dependency are currently not well understood.

IV. Conclusion and Future Work

A theoretical model is derived that allows the determination of the thermal diffusivity of a cantilever microbeam using the optical beam deflection method. Via this non-contact, non-destructive method also the effective conductance and the layer thicknesses can be determined if the material properties are known. Initial experimental results show that proposed method is capable of resolving the thermal diffusivity of microcantilevers. Experiments conducted in vacuum conditions are required for full validation of the theoretical model.

Acknowledgment

This research was financially supported by enabling technology program Materials. Special gratitude goes to dr. Rodolf Herfst for his help on the experimental table-top AFM setup used in this research.

 ISBN: 978-1-61208-297-4

APPENDIX

The transfer function for the rotation of the cantilever due to a local heat input is given by

$$\begin{aligned} G(s) = \frac{\sqrt{2\pi}c}{8(s+B)\cosh(k_3)}\{ & \\ & -2\exp(k_1)[\operatorname{erf}(\mathrm{m}_1)+\operatorname{erf}(\mathrm{m}_2)] \\ & +2\exp(k_2)[\operatorname{erf}(\mathrm{m}_4)-\operatorname{erf}(\mathrm{m}_3)] \\ & \quad +4\cosh(k_3)\operatorname{erf}(\mathrm{m}_5) \\ & +\exp(k_4)[\operatorname{erf}(\mathrm{m}_3)-\operatorname{erf}(\mathrm{m}_4)] \\ & +\exp(k_5)[\operatorname{erf}(\mathrm{m}_2)+\operatorname{erf}(\mathrm{m}_4)] \\ & +\exp(k_6)[\operatorname{erf}(\mathrm{m}_3)-\operatorname{erf}(\mathrm{m}_1)] \\ & \quad +\exp(k_7)[\operatorname{erf}(\mathrm{m}_1)+\operatorname{erf}(\mathrm{m}_2)]\} \end{aligned}$$

where the auxiliary parameters are given by:

$$k_1 = \frac{2D(b-L)\sqrt{\frac{s+B}{D}}+(s+B)c^2}{2D}$$

$$k_2 = \frac{2D(b-L)\sqrt{\frac{s+B}{D}}+(s+B)c^2}{2D}$$

$$k_3 = \sqrt{\frac{s+B}{D}}L$$

$$k_4 = \frac{2D(L-2b)\sqrt{\frac{s+B}{D}}+(s+B)c^2}{2D}$$

$$k_5 = \frac{-2DL\sqrt{\frac{s+B}{D}}+(s+B)c^2}{2D}$$

$$k_6 = \frac{2DL\sqrt{\frac{s+B}{D}}+(s+B)c^2}{2D}$$

$$k_7 = \frac{2D(2b-L)\sqrt{\frac{s+B}{D}}+(s+B)c^2}{2D}$$

$$m_1 = \frac{\sqrt{2}\left(b+c^2\sqrt{\frac{s+B}{D}}\right)}{2c}$$

$$m_2 = \frac{\sqrt{2}\left(L-b-c^2\sqrt{\frac{s+B}{D}}\right)}{2c}$$

$$m_3 = \frac{\sqrt{2}\left(L-b+c^2\sqrt{\frac{s+B}{D}}\right)}{2c}$$

$$m_4 = \frac{\sqrt{2}\left(-b+c^2\sqrt{\frac{s+B}{D}}\right)}{2c}$$

$$m_5 = \frac{\sqrt{2}}{2}\frac{b}{c}$$

REFERENCES

[1] W. Young and R. G. Budynas, *Roark's Formulas for Stress and Strain*, 7th ed. New York: McGraw-Hill, 2002.

[2] B. Bardes, H. Baker, W. Cubberly, and A. I. Committee, *Metals Handbook*, 9th ed., B. Bardes, P. Baker, Hugh, Cubberly, and William, Eds. American Society for Metals, 1978.

[3] C. Gibson, D. Smith, and C. Roberts, "Calibration of silicon atomic force microscope cantilevers," *Nanotechnology*, vol. 16, pp. 234–238, 2005.

[4] J. Jou, C. Liao, and K. Jou, "A method for the determination of gold thin film's mechanical properties," *Thin Solid Films*, vol. 238, pp. 70–72, 1994.

[5] Y. Ju, "Phonon heat transport in silicon nanostructures," *Applied Physics Letters*, vol. 87, p. 153106, 2005.

[6] W. Liu and M. Asheghi, "Phonon-boundary scattering in ultrathin single-crystal silicon layers," *Applied Physics Letters*, vol. 84, p. 3819, 2004.

[7] S. Okuda, M. Kobiyama, and T. Inami, "Mechanical Properties and Thermal Stability of Nanocrystalline Gold Prepared by Gas Deposition Method," *Materials Transactions, JIM*, vol. 40, no. 5, pp. 412–415, 1999.

[8] D. Son, J. Jeong, and D. Kwon, "Film-thickness considerations in microcantilever-beam test in measuring mechanical properties of metal thin films," *Thin Solid Films*, vol. 437, pp. 182–187, 2003.

[9] S. Sheng, A. Narayanaswamy, S. Goh, and G. Chen, "Thermal conductance of bimaterial microcantilevers," *Applied Physics Letters*, vol. 92, no. 063509, 2008.

[10] H. Sadeghian and R. Herfst, "Systematic characterization of optical beam deflection measurement for micromechanical systems," *unpublished*.

[11] M. Kasper, V. Natrajan, N. Privorotskaya, K. Christensen, and W. King, "Natural advection from a microcantilever heat source," *Applied Physics Letters*, vol. 96, p. 063113, 2010.

[12] K. Kim and W. King, "Thermal conduction between heated microcantilever and a surrounding air environment," *Applied Thermal Engineering*, vol. 29, pp. 1631–1641, 2009.

 ISBN: 978-1-61208-297-4